PROCEEDINGS/PART 1

FALLOUT PHENOMENA SYMPOSIUM

APRIL 12-14, 1966

Sponsored by

DEFENSE ATOMIC SUPPORT AGENCY

OFFICE OF CIVIL DEFENSE

at

THE NAVAL POSTGRADUATE SCHOOL
Monterey, Calif.

Technical Assistance by
THE TECHNICAL MANAGEMENT OFFICE

US NAVAL RADIOLOGICAL DEFENSE LABORATORY
SAN FRANCISCO, CALIFORNIA

DASA MISSION

J. W. Cane
Defense Atomic Support Agency
Washington, D.C.

Good Morning Gentlemen:

I would like to welcome you, on behalf of DASA, to this symposium. I was personally gratified by the response to invitations. This symposium was originally intended to be an exchange of views between OCD and DASA Contractors, but it soon became apparent that the attendance should not be limited to them, and we are pleased at the great interest shown in this meeting.

The DASA mission is to support the Secretary of Defense, Joint Chiefs of Staff, Services and others as appropriate in nuclear weapons matters. Primary staff supervision comes from JCS while DDR&E has cognizance over our RDT&E programs. In addition, ATSD (AE) supervises certain of our logistics, safety and liaison activities. We are the DOD Coordinator for research in the effects of nuclear weapons, and we respond to requirements of the Services for effects information. This boils down to the following with regard to fallout research: We sponsor research activity which we in coordination with the services feel to be necessary to enable one to adequately assess the fallout hazard as it affects military operations and strategic plans. Our current program is at a focus. We are completing the first version of the DOD land fallout prediction system this year. You will hear more about this later in the symposium. We expect this model to provide all users with the type of information they need, but also, and just as important for this group, we expect tests of this model to tell us what effects are the most significant contributors to fallout prediction, so that with these results we can go ahead and simplify the model in those areas where tests show it is advisable, and do more research in those areas where

we need more complete knowledge. So, the results of future tests of the completed model will determine the direction of our effort. This is the reason for my earlier remark about our program coming to a focus.

In addition to the DOD fallout prediction system, we have in final stages of completion prediction codes for underwater and water surface bursts and for fast-neutron activation of soil materials. We are proceeding with publication of DASA 1215, the five-volume compilation of fallout data from past shots. We also have a pilot program of post facto cloud filter analysis, of which you will hear more later.

Before yielding the floor to Mr. Greene, may I leave two thoughts with you: First, please remember we are allotting 1/2 day for each session and discussion in order to be finished in two days; second, I am looking forward to a most interesting symposium. In this connection may I borrow from John Milton the following quotation to keep our sessions in perspective: "Where there is much desire to learn there of necessity will be much arguing, much writing, many opinions; for opinion in good men is but knowledge in the making."

EXPERIMENTAL DETERMINATION OF INPUT FOR THE PREDICTION OF FRACTIONATION EFFECTS

E. C. Freiling
U.S. Naval Radiological Defense Laboratory
San Francisco, California

ABSTRACT

The lack of uniformity in radiochemical composition among samples of nuclear debris produces a concomitant variation in many properties of interest: the partition of radionuclides among local, tropospheric, and stratospheric fallout, the exposure rate from deposited debris, the variation of this rate with shielding and rainwater leaching, and the availability of individual nuclides to the biosphere. The recognition of the importance of these effects has produced a demand for increasing sophistication in the methods of predicting them. Our work at NRDL is presently concerned with the theoretical development of a kinetic method for the prediction of fractionation effects and the simultaneous measurement of required kinetic and thermodynamic input data.

Using a two-temperature furnace of special design, the rates of condensation of MoO_3 vapor on calcium ferrite, sodium silicate, calcium aluminum silicate eutectic, and clay loam have been measured. Experiments were performed at 1400°C in dry air at partial pressures of $5x10^{-7}$ to $5x10^{-4}$ atm. of MoO_3. Uptake for spherical particles was determined as a function of time and particle diameter. Both rate and mechanism of uptake were found to vary markedly with substrate composition.

CONCLUSION

If the rate-controlling steps observed here hold for the conditions under which particles are formed in Nevada and Eniwetok, these results have considerable practical significance. To the already impressive list of known differences between Nevada and Eniwetok surface shots (viz., yield, soil melting point, soil boiling point, chemical affinity) they add the difference of mechanism of condensation for at least one fission product element. Attendant to this possibility is the awareness that added caution is necessary when extrapolating results from one soil to another, particularly when so many difficulties in fallout prediction, past and present, can be traced to one or another unwarranted extrapolation.

There is some slight evidence that such a difference in mechanisms may hold under actual shot conditions. Russell[4] has pointed out that, in the 5 to 50-μ range of active particles from Bravo, Sr^{89} was incorporated as the 1.4 power of the diameter and Mo^{99} as the 1.8 power, while in undifferentiated Johnie Boy debris these powers were 2.0 and 2.8 respectively. Of course, the behavior we have observed would be more appropriately applied to Ru and Rh activities, but the differences mentioned by Russell are at least cause for concern.

Further studies are necessary to determine whether these results hold at the lower vapor pressures, smaller particle sizes and higher temperatures prevailing in fallout formation. Table 2 shows some of the effects that changes in conditions may produce. Also necessary are observations on the effect of water vapor, comparison of ambiguous cases with theoretical equations, and comparison of apparently clear cut cases to measured diffusion constants.

In closing it is appropriate to paraphrase the words of G. N. Lewis and M. Randall in their classic treatise on thermodynamics: "Let this (work) be dedicated to the (fallout scientists) of the newer generation, who will not wish to reject all inferences from conjecture or surmise,

REFERENCES

1. J. P. Hirth and G. M. Pound, "Condensation and Evaporation. Nucleation and Growth Kinetics." Volume 11 of "Progress in Materials Science," B. Chalmers, Ed., Pergamon Press, MacMillan, New York, 1963.

2. E. C. Freiling, G. R. Crocker and C. E. Adams, "Nuclear-debris Formation," p. 1 of "Radioactive Fallout from Nuclear Weapons Tests," Proceedings of the Second Conference, 3-6 November 1964, A. W. Klement, Jr., Ed., USAEC Division of Technical Information, November 1965.

3. J. H. Norman, et al., "Fallout Studies--Cloud Chemistry," Final Report, GA 6094, 29 January 1965.

4. I. J. Russell, private communication.

COMPARISON OF NUCLEAR FALLOUT MODELS*

M. Polan
Ford Instrument Company
Long Island City, N.Y.

ABSTRACT

The fallout prediction models presented at the 1962 USNRDL-DASA Fallout Symposium will be discussed. They include those developed or used by the following agencies: RAND Corp. (simplified version), Weapon Systems Evaluation Group, Defense Intelligence Agency, National Resource Evaluation Center (Dusty III), NRDL (D and Miller-Anderson), Ford Instrument Co. (T), Technical Operations Research, University of California Civil Defense Research Project and Lawrence Radiation Laboratory (Dr. Knox's and Dr. Shelton's), U.S. Army, U.S. Navy (RADFO), U.S. Weather Bureau, Sandia Corp. (Dropsy), AN/GMQ-18, AN/GMQ-21, and U.S. Army Signal Corps, most of which are currently considered valid.

The models simulate the transport and deposition of fallout in one or the other of two ways:

1. A single effective fallout wind (EFW) is used to simulate the horizontal wind field, and the size and shape of the fallout contours are a function (explicit or implicit) of this EFW and the yield.

2. A multilayer wind field is used, the nuclear cloud is partitioned (by horizontal slicing and by grouping of particle sizes) into small elements (wafers), and the trajectory of each wafer is computed.

The EFW models are found to be suitable for use when computing-speed requirements outweigh the accuracy requirements (multiburst operations analysis and military field operations). The wafer models are found to be suitable when the requirements are reversed (in scientific, engineering, and military studies, including predicting fallout at nuclear test sites).

*Based on work performed for USNRDL under contract No. N228(62479)62185, Bureau of Ships Subproject SF 011 05 12, Task 0506.

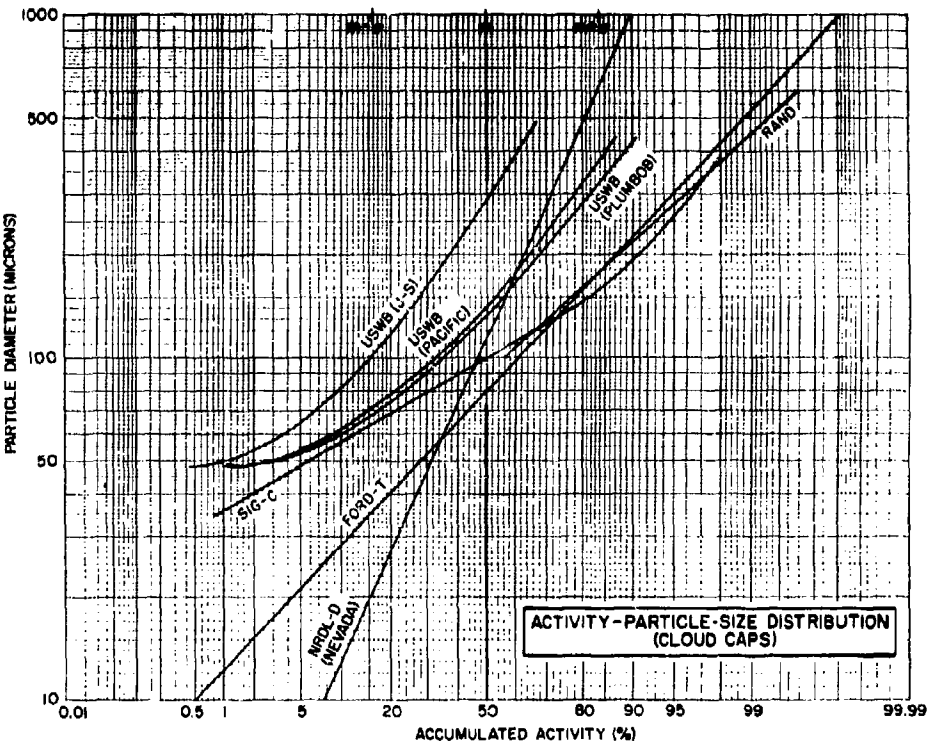

Fig. 8. Activity-Particle-Size Distribution (Cloud Caps)

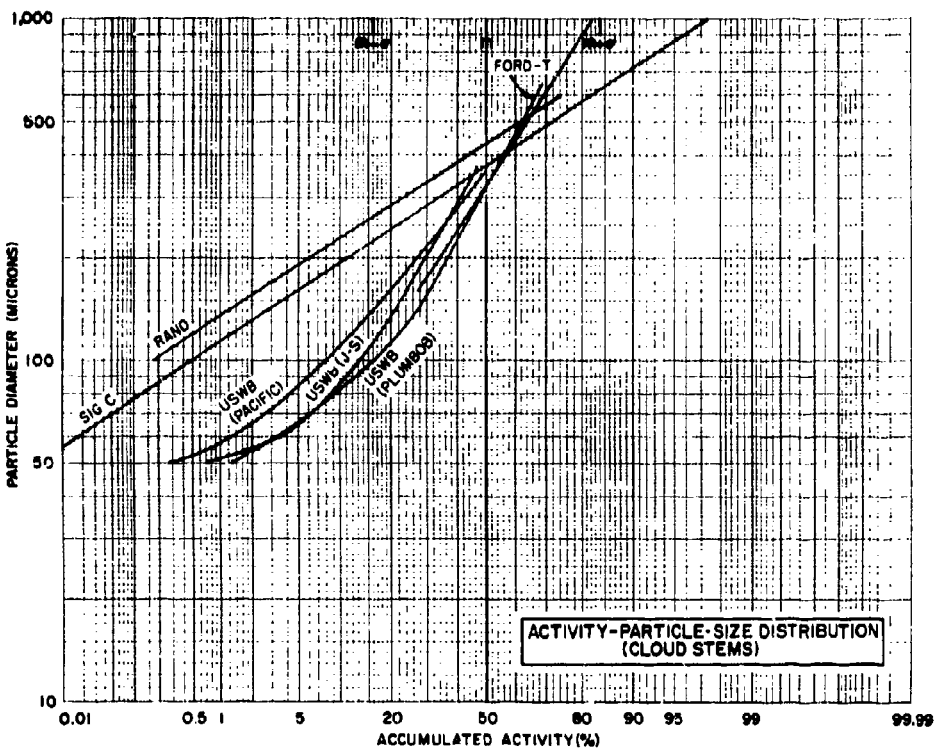

Fig. 9. Activity-Particle-Size Distribution (Cloud Stems)

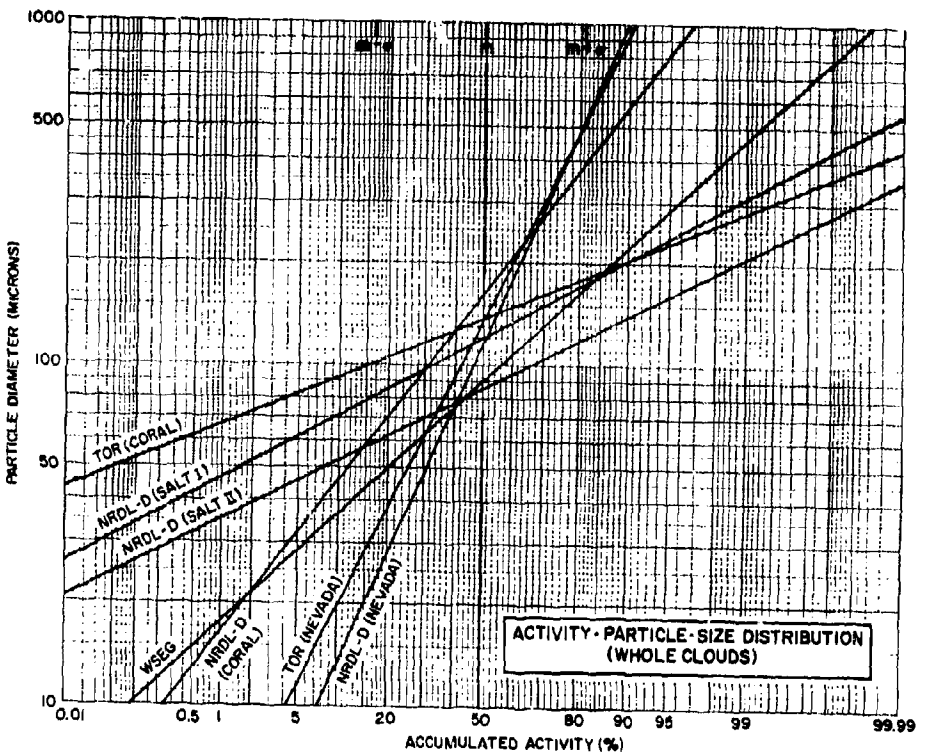

Fig. 10. Activity-Particle-Size Distribution (Whole Clouds)

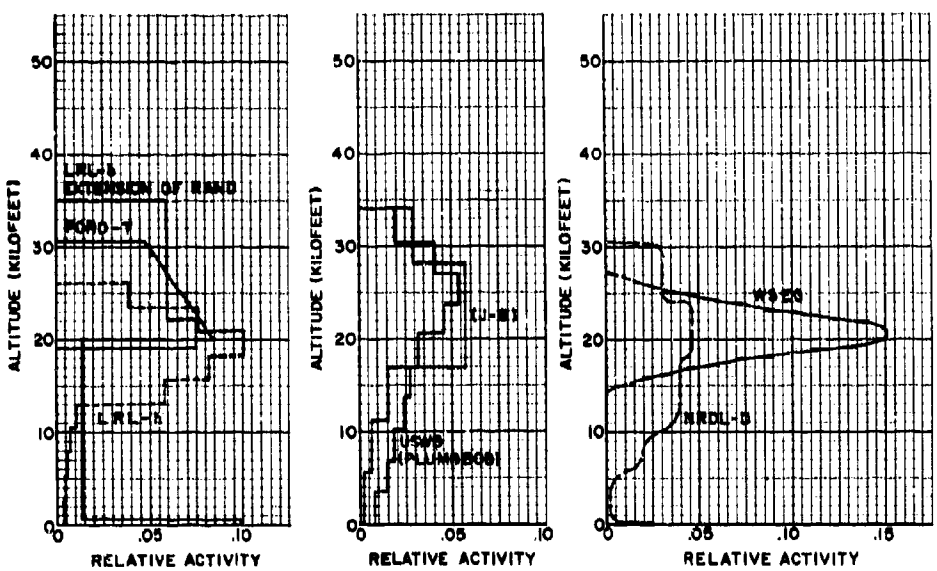

Fig. 11. Vertical Distribution of Activity for a Land-Surface Blast at MSL (20-KT Yield)

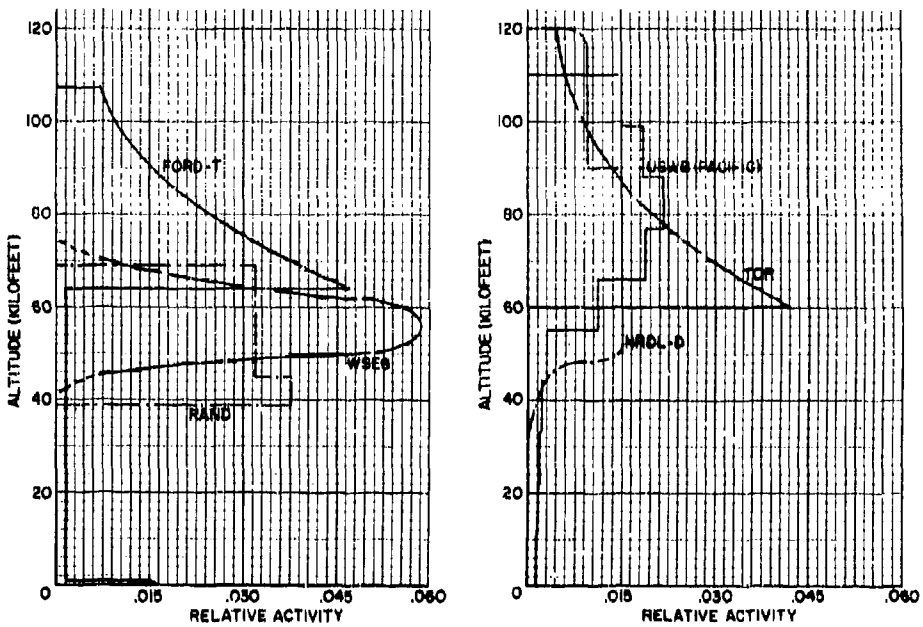

Fig. 12. Vertical Distribution of Activity for a Land-Surface Blast at MSL (20-MT Yield)

NORMALIZATION FACTORS

Model	NF (r /hr per KT/sq.st.mile)	
	Ideal Plane	Realistic Flat Terrain
RAND	1200-2660	----
WSEG	2400	----
NREC, CDRP	2500	----
TOR	1580	870
Ford-T	1200	900
NRDL-D	1682	1093
LRL-h,LRL-b	3380	2700
Signal Corps.	984	689
USWB	1500	1050
Dropsy	2585	----
DIA	1100	**

Fig. 13. Normalization Factors

GAMMA RAY FIELDS ABOVE ROUGH CONTAMINATED SURFACES

R. R. Soule
U.S. NAVAL RADIOLOGICAL DEFENSE LABORATORY
San Francisco, California

ABSTRACT

The object of this experiment is to determine the gamma radiation fields above uniformly contaminated surfaces of infinite extent and varying roughness.

Radioactive contaminant (Au^{198} suspended in glass microbeads) was distributed evenly over a circular area 10 ft in diameter in the center of various test surfaces. Ionization chambers were employed to measure the radiation field at various distances out to 128 meters horizontally and 16 meters vertically from the center of the area. These data were then operated upon to obtain the radiation fields to be expected from surfaces of infinite extent. Comparisons of the results from a given surface with those obtained from an ideally smooth (glass) plane provide a measure of surface roughness. Surfaces tested included sand, gravel and grass.

The theory and assumptions used in integrating the data from the finite discs to determine the fields for infinite planes are presented. Preliminary examination of the data from the experimental work indicates the following results:

Surface Roughness Factors for Test Surfaces
at a Height of 1 Meter Above the Surfaces

Surface	Infinite Plane Dose Rate (r/hr)/(c Au^{198}/ft^2)	Surface Roughness Factor
Plate Glass	77.0	1.00
Grass (wet)	61.0	0.79
Coarse Sand	50.3	0.65
Fine Gravel	47.7	0.62
Pea Gravel	42.9	0.56
Medium Gravel	44.5	0.58

Measurements were also made with a point source of Au^{198}. Buildup factors derived from these measurements are presented.

Recent experimentation has been performed at the Camp Parks Facility of the Naval Radiological Defense Laboratory to determine the effect of surface roughness upon gamma ray fields. The objective of this experimentation is to determine the gamma radiation fields above uniformly contaminated surfaces of infinite extent and varying roughness.

In this experimentation[1] radioactive contaminant is spread over a circular area 10 feet in diameter in the center of various test surfaces. Measurements of the radiation field are taken at predetermined distances horizontally and vertically from the center of the area. These data are then operated upon to obtain the radiation fields to be expected from surfaces of infinite extent. Comparison of the results from a given surface with those obtained from an ideally smooth (glass) plane provide a measure of surface roughness.

In order to fully expose the assumptions and limitations inherent in the extrapolation from a finite disc to an infinite field, the scheme used is developed below.

A disc of finite size may be used to approximate a uniformly contaminated plane. The disc is large (dia. 10 ft) in relation to the irregularities which characterize the roughest surfaces used, but is small enough to facilitate the handling and control of the radioactive contaminant. The radiation field (R_0) measured above the center of the contaminated disc is the first term in a series approximation to the field (R) above an infinite plane. The second term in the series is obtained by taking the radiation contribution (R_1) from an annulus (1 disc diameter in width) adjoining the disc. Successive terms are composed of the radiation contributions (R_2, R_3, ...R_n) from additional adjoining annuli. The approximation of the radiation field due to a contaminated infinite plane becomes better as the number of annuli increase.

$$R \approx R_0 + R_1 + R_2 + \ldots R_n \qquad (1)$$

If the radiation contribution (r_n) from a sector of an annulus is known, the contribution (R_n) from the entire annulus can be found by multiplying the sector contribution by b_n, where b_n is defined as the ratio of the area of the annulus to the area of the sector.

$$R_n = b_n r_n, \quad b_n \equiv \frac{\text{area of annulus } n}{\text{area of sector}} \quad \text{for } n \geq 1$$

If the sector of an annulus 1 disc diameter wide is chosen to have the same area as a disc of the chosen diameter, the coefficients b_n are simply multiples of 8, and the approximation can be expressed as

$$R \approx R_0 + 8r_1 + 16r_2 + 24r_3 + \cdots + 8nr_n \qquad (2)$$

The radiation contribution (c_n) from a disc of the chosen diameter, contained within the annulus, can be used to approximate the radiation contribution (r_n) from the sector of the annulus. Differences in the actual contributions of the disc and the sector can be adjusted by the use of a correction factor k_n, where k_n is defined to be the ratio of the radiation contribution of a sector to the radiation contribution of a disc.

$$r_n = k_n c_n, \quad k_n \equiv \frac{\text{radiation contribution from sector}}{\text{radiation contribution from disc}} \quad \text{for } n \geq 1$$

and then $$R_n = 8nr_n = 8nk_n c_n \qquad (n \geq 1) \qquad (3)$$

The values of the correction factors k_n were determined by calculating the radiation contributions from elemental areas of both the disc and the sector, summing for each, and finding the ratio of the sums for a smooth plane. The circle was divided into areas a_1, a_2, a_3, $\cdots$ a_m, and the sector into areas s_1, s_2, s_3, $\cdots$ s_m, at mean horizontal distances d_1, d_2, d_3, $\cdots$ d_m from the detector (See Fig. 1). If the response of a detector at a height h is 1 unit/unit area at unit distance, the response due to the circle will be

$$c_n = \frac{a_1}{h^2+d_1^2} B_1 e^{-\mu d_1'} + \frac{a_2}{h^2+d_2^2} B_2 e^{-\mu d_2'} + \cdots \frac{a_m}{h^2+d_m^2} B_m e^{-\mu d_m'} \qquad (4)$$

where B is the buildup factor, $e^{-\mu d'}$ is due to air attenuation, and $\frac{1}{h^2+d^2}$ is the geometrical factor. The slant range $d' = (h^2+d^2)^{1/2}$. The response due to the sector will be

$$r_n = \frac{s_1}{h^2+d_1^2} B_1 e^{-\mu d_1'} + \frac{s_2}{h^2+d_2^2} B_2 e^{-\mu d_2'} + \cdots + \frac{s_m}{h^2+d_m^2} B_m e^{-\mu d_m'} \qquad (5)$$

The correction factor for the disc approximation of the sector contribution to the radiation field will be

$$k_n = \frac{\sum_{i=1}^{m} \frac{s_i}{h^2+d_i^2} B_i e^{-\mu d_i'}}{\sum_{i=1}^{m} \frac{a_i}{h^2+d_i^2} B_i e^{-\mu d_i'}} \qquad (6)$$

The dimensions of the disc and the sector are such that changes in the air attenuation and buildup factors are small for changes of less than 1 disc diameter in the horizontal distance to the detector. Thus, buildup and air attenuation can be assumed constant for each k_n determination, and k_n becomes

$$k_n = \frac{\sum_{i=1}^{m} \frac{s_i}{h^2+d_i^2}}{\sum_{i=1}^{m} \frac{a_i}{h^2+d_i^2}} \qquad (7)$$

The expression $\sum_{i=1}^{m} \frac{a_i}{h^2+d_i^2}$ cannot be easily evaluated analytically so it was evaluated numerically. However the expression $\sum_{i=1}^{m} \frac{s_i}{h^2+d_i^2}$

approaches $\int_{r_1}^{r_m} \int_{0}^{\pi/4n} \frac{r\, d\theta\, dr}{h^2 + r^2}$ as the width of the elemental areas approaches zero. Analytical evaluation of the latter expression gave results which agreed to within 0.01% with the numerical evaluation of $\sum_{i=1}^{m} \frac{s_i}{h^2+d_i^2}$

The values of k_n were determined for the case of a detector located at a height of 1 meter and for disc diameter and annuli widths of 10 ft (See Figure 1). The value of k_1, for the first annulus, was found to be 0.949, k_2 was found to be 0.989, and the values of k_n for $n>2$ were taken to be unity.

The final form of the approximation of the infinite plane radiation field then becomes

$$R = R_0 + 8(0.949)c_1 + 16(0.989)c_2 + 24c_3 + 32c_4 + \ldots + 8nc_n \qquad (8)$$

where R_0 is the measured radiation contribution above the center of a 10 ft diameter contaminated disc, and c_n is the radiation contribution measured at a horizontal distance of 10n ft from the center of the disc (all measurements made at a height of 1 meter).

The basic experiment consists of measuring the total gamma radiation field at selected heights and distances from contaminated discs of materials of varying degrees of roughness. Gamma measurements are made using ionization chambers. Data from these measurements are extrapolated (integrated) to predict the dose rate for infinite plane sources.

The test surfaces used during this series of experiments were:

1. Plate glass - a smooth surface.
2. Coarse sand (1190 - 2000 μ particle size) (3/64 - 1/64 inches)
3. Fine gravel (2362 - 5613 μ particle size) (3/32 - 7/32 inches)

4. Pea gravel (6680 - 9423 μ particle size) (1/4 - 3/8 inches)
5. Medium size gravel (13,330 - 15,585 μ particle size) (1/2 - 5/8 inches)
6. Grass (lawn type)

The isotope used for this series was Au^{198}, a gamma emitter with an energy of 0.411 Mev. The isotope, enclosed in a microbead carrier, was uniformly dispersed at a mass loading of approximately 12 grams/sq. ft over a 10 ft diameter disc in the center of the test surfaces.

The basic gamma measurements were taken with ionization chambers at combinations of horizontal distances from 0 to 128 meters and vertical distances from 1 to 16 meters from the center of the test surface.

The data from the tests where the isotope was dispersed uniformly over the "ideally smooth surface" (plate glass) was taken as the basis for comparison with the other surfaces of varying roughness. Thus the surface roughness factor depends on the determination of a smooth surface infinite plane exposure as well as on a rough surface infinite plane exposure.

If certain factors, such as the build-up factors, are known, the smooth surface exposure can be calculated to provide a check on the experimentally obtained smooth surface exposure values. Since the experiment was concerned with the region close to the ground-air interface, it was not reasonable to use the infinite medium build-up factors available. For this reason, a supplemental test was conducted in which a series of measurements were made using a gold wire as a point source for the purpose of determining the build-up factor for Au^{198} under the conditions of the experiment.

The gold wire was 5 cm long by 0.095 cm in diameter. All radiation measurements were made in a direction normal to the axis of the wire. The diameter and cross section of the wire were chosen to minimize self-absorption and eliminate angular dependence of gamma rays emitted

perpendicular to the axis of the wire. The length of the wire was selected so that it was long enough to provide the required source strength and yet short enough so that no appreciable error was introduced in considering the wire as a point source at the minimum measurement distance of one meter.

The wire was irradiated to produce an initial activity of about 100 curies. The wire was then placed upon the glass plate in the center of the test pad and radiation field measurements were made at distances from 1 meter to 128 meters from the source at heights of 1, 4, 8, and 16 meters above the plane of the glass plate.

The build-up factors as a function of position of the detector were determined from the expression $I = I_o \frac{e^{-\mu_o r}}{r^2} B$ where I is the intensity in r/hr at the detector position, I_o is the intensity at unit distance from the source in an infinite medium of air, μ_o is the total attenuation coefficient and B is the build-up factor.

Experimentation was conducted on a test surface located at the intersection of two streets which are paved with asphaltic concrete. There are no buildings in the area. A level concrete pad, 30 ft square, was constructed at the intersection of the streets. The central 15 ft square section was further leveled by grinding the surface flat to within ± 1/8 inch, and the test surfaces were centered in this area. For the smooth surface, six sections of 1/4 inch thick plate glass were arranged horizontally on a 1/4 inch thick sponge rubber pad and leveled to provide a smooth level test surface 11 ft square.

For the rough surfaces, a sheet of 5 mil thick plastic was placed on the plate glass surface and the loose material was spread on it. (Figure 2.) A single layer technique was used in spreading the sand and gravel test surfaces. No binder was used, and the intent was to spread a single layer of the sand or gravel and then add additional material

until no visible holes remained in the layer. This resulted in a layer of the material only slightly thicker than the maximum size of the material.

Because the test area is in the open, a plastic dome was constructed to cover the test surface and prevent the wind from moving the contaminant. The dome is approximately 14 ft square by 3 ft high, and the 3 mil thick Mylar sheeting is supported by an aluminum framework that provides a clear span across the entire width. Since the dome is kept in place over the test surface at all times, one end of the dome is hinged to allow for the entrance and removal of the contaminant and the contaminant dispersal equipment.

The source of radiation for all the tests was the isotope Au^{198}. The radioactive isotope was enclosed in a microbead carrier for the tests in which it was dispersed uniformly over the various test surfaces, and was a single piece of metallic gold for the point source tests. The beads were taken to the test area in a shielded container from which they were delivered into a disperser (Figure 3).

The disperser that distributes the microbeads onto the test surface is a hopper mounted on a small portable motorized bridge crane. As the hopper moved from one side of the area to the other, an auger bit in the bottom of the hopper provided a continuous flow of the microbeads at a constant dispersal rate through four outlets. Four baffles below the outlets spread the microbeads to give an even distribution on the test surface.

The size of the contaminated area was controlled by a mask that rested on the framework of the disperser assembly below the level of the hopper and baffles. Eight aluminum pans were fitted together to form the mask to control the size and shape of the contaminated area (Figure 4). The mask had outside dimensions of an 11 ft 10 inch square and had a 10 ft diameter circular cut-out in the center. As the hopper moved from one side of the disperser to the other, the

contaminant fell on the test surface inside the circle while the mask caught the excess. Complete coverage inside the circle was obtained by first dispersing along one side of the mask and indexing the hopper over one hopper width after each pass. After the dispersal of the contaminant, the disperser, including the hopper and mask containing the excess contaminant, was removed from under the plastic dome, and the hinged end of the dome was closed for the duration of the test. The excess contaminant was removed from the test area and measurements were started using Victoreen ionization chambers mounted on a light portable mast (Figure 5).

Preliminary results are available from the experimental work. Figure 6 shows the build up factors derived from data measured with the point source of Au^{198}. It is interesting to note that the 16 meter height factors are below those for heights of 4 and 8 meters.

Figures 7 and 8 present data for the pea gravel surface and grass surface typical of those obtained during the experiments. This type of data was used in conjunction with equation 8 to obtain the infinite plane exposure rates at 1 meter above the surface. Comparison of the various surfaces with the glass surface gave measures of surface roughnesses. The infinite plane exposure rates and the roughness factors are given in Table 1.

A small amount of additional experimental work will be done to obtain an indication of the effect of gamma ray energy upon surface roughness factors. Lutetium-177 with a gamma energy of about .200 mev will be employed on two or three surfaces for this purpose. Point source measurements will also be made with the Lu^{177}.

Table 1

Surface Roughness Factors for Test Surfaces at a Height of 1 Meter Above the Surfaces

Surface	Infinite Plane Exposure Rate (r/hr)/c Au^{198}/ft^2	Surface Roughness Factor
Plate Glass	77.0	1.00
Grass	61.0	0.79
Coarse Sand	50.3	0.65
Fine Gravel	47.7	0.62
Pea Gravel	42.9	0.56
Medium Gravel	44.5	0.58

REFERENCES

1. Kehrer, W. S., et al., Gamma Ray Fields Above Rough Contaminated Surfaces. Progress to 31 January 1966. USNRDL-Letter Report in preparation.

GENERAL REFERENCES

1. Ksanda, C. F., A. Moskin, E. S. Shapiro, Gamma Radiation From a Rough Infinite Plane, USNRDL-TR-108, 18 January 1956.
2. Spencer, L. V., Structure Shielding Against Fallout Radiation From Nuclear Weapons, U.S. Department of Commerce, National Bureau of Standards, Monograph 42, 1 June 1962.
3. Ferguson, J. M., Ground Roughness Effects for Fallout-Contaminated Terrain: Comparison of Measurements and Calculations, USNRDL-TR-645, 7 May 1963.
4. Triffet, T., P. D. LaRiviere, Characterization of Fallout, Operation REDWING (U), WT-1317, 1961 (Secret-RD).
5. Clifford, C. D., Effects of the Ground on the γ Dose From Distributed ^{137}Cs Sources, Canadian Journal of Physics, Vol. 42, pp. 2373-2383, 1964.
6. Huddleston, C. M., et al, Ground Roughness Effects on the Energy and Angular Distribution of Gamma Radiation From Fallout, U.S. Atomic Energy Commission, CEX 62.81, July 1964.
7. Schlemn, C. L., et al, Scattered Gamma Radiation Measurements From a Co^{60} Contaminated Field, AFSWC-TN-59-6, 1959.
8. Mahoney, J. J., R. B. Price, Experimental Tests of Shielding and Attenuation of Gamma Radiation From Radioactive Tantalum Versus Infinite Plane Theory, CRLIR 94, 1952.
9. Strope, W. E., Evaluation of Countermeasure System Components and Operation Procedures, WT-1464, 1958.
10. Starbird, A. W., J. F. Batter, Angular Distribution of Skyshine Radiation at the Surface of a Place of Fallout Contamination, Technical Operations Research, TO-B 63-40, March 1964.
11. Mather, R. L., et al, Gamma Radiation Field Above Fallout Contaminated Ground, WT-1225, 1959.

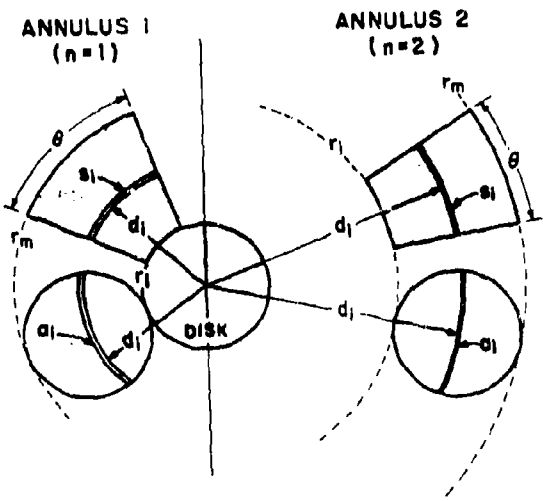

Fig. 1. Disc and Sector Used in Determining the Radiation Contribution From a Sector of a Contaminated Annulus

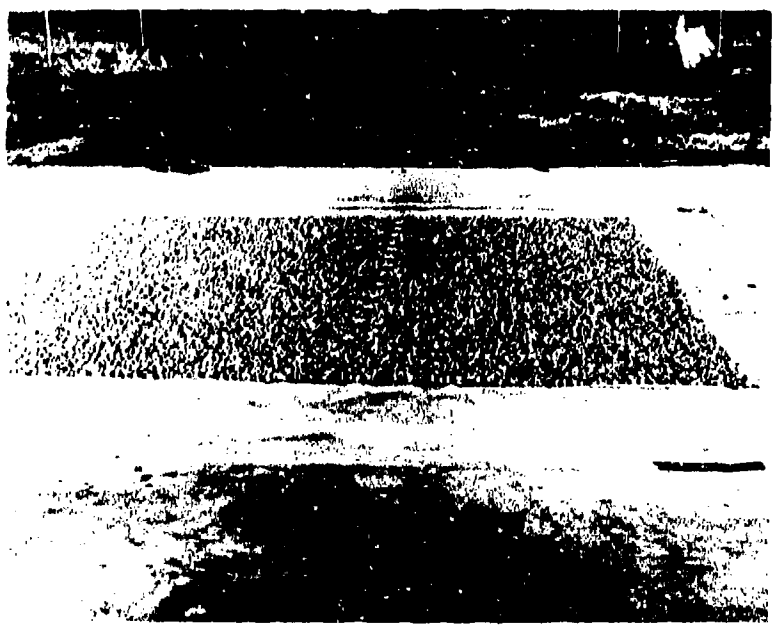

Fig. 2. Medium Gravel Test Surface

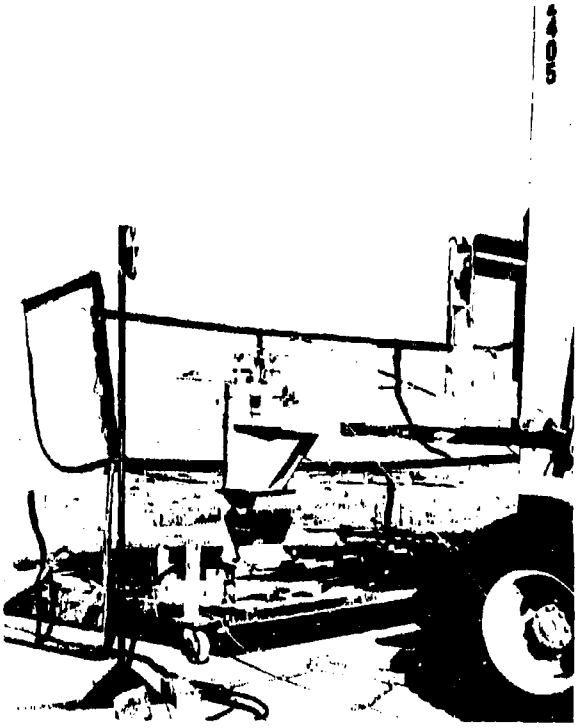

Fig. 3. Shielded Container and Contaminant Disperser

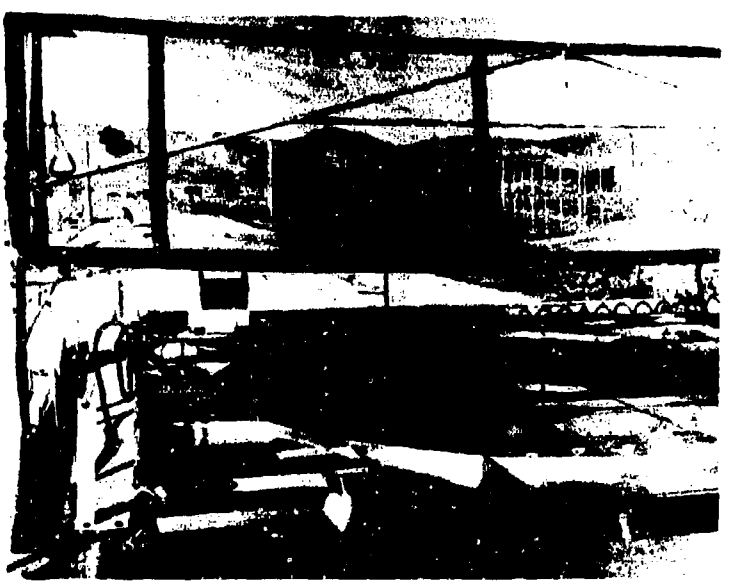

Fig. 4. Disperser and Circular Mask

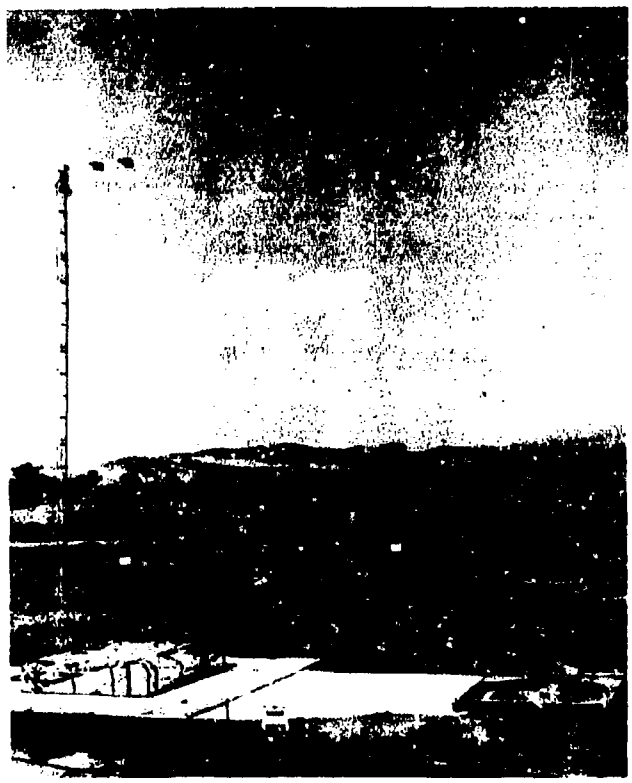

Fig. 5. Test Surface and Instrument Mast

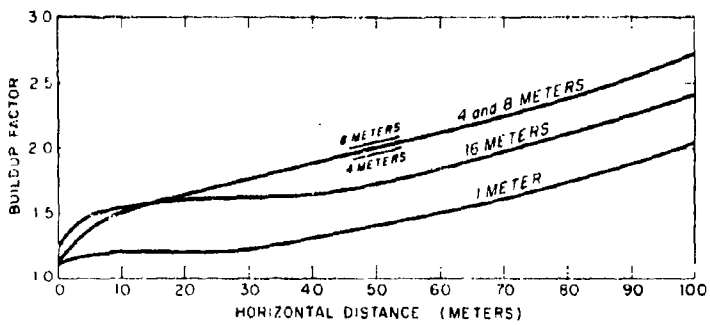

Fig. 6. Buildup Factors vs Horizontal Distances at Vertical Distances of 1,4,8 and 16 Meters Point Source at Au^{198} of Plate Glass Surface

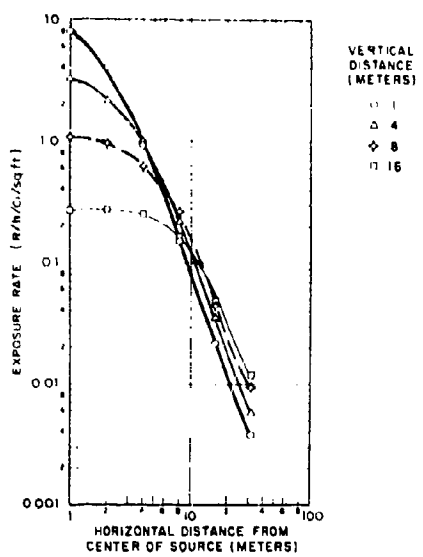

Fig. 7. Exposure Rate from 10 ft Diameter Disc of Au^{198} Contaminant on a Pea Gravel Surface

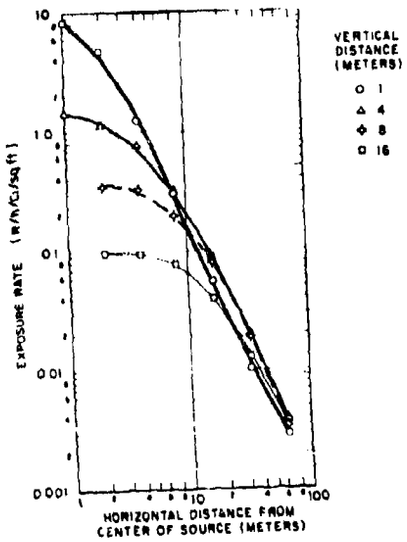

Fig. 8. Exposure Rate from 10 ft Diameter Disc of Au^{198} Contaminant on a Grass (Lawn Type) Surface

DISINTEGRATION RATE MULTIPLIERS IN BETA EMITTER DOSE CALCULATIONS*

S. L. Brown
Stanford Research Institute
Menlo Park, California

ABSTRACT

The possible biological doses from external beta emitters will be discussed and compared with those from external gamma emitters. A detailed analysis has been made of the dose distribution in tissue to be expected from individual beta-emitting radionuclides in contact dose or beta bath plane geometries. In the former case, a thin plane source is sandwiched between two semi-infinite media, the absorber and the back-scatterer. For the latter case, a third medium, an attenuator of finite thickness, is introduced between the backscatterer and absorber, with the source between the backscatterer and attenuator. Point isotropic dissipation functions due to Spencer were integrated over the plane and corrected for backscatter using his plane perpendicular functions.(6) These functions are given for monoenergetic electrons; hence another integration was performed over the beta energy spectrum for each radionuclide. Spectra for nearly 400 beta-emitting radionuclides have been taken from calculations of Hogan, Zigman, and Mackin.(7) Disintegration rate multipliers, which convert contamination levels in dis/sec/cm^2 to dose rates in rad/sec, have been calculated for these radioisotopes for several depths in tissue and widths of air gap. Simplified models based on the beta end-point energy will also be discussed and comparisons will be made with the simplified results and with a simplified gamma model. The conclusion to be offered is that beta radiation can be a serious hazard in comparison with gamma radiation if there are unprotected radiosensitive tissues at shallow depths in the exposed organism.

*Research supported by the Office of Civil Defense.

Table 3

Beta and Gamma Dose Rates From Fission Product Contamination

Case 1		Case 2	
2.1×10^{17} fissions		2.1×10^{19} fissions	
1.95×10^{12} fissions/sq ft		1.95×10^{14} fissions/sq ft	
1.48	r/hr @ 1 hr	1.48×10^{2}	r/hr @ 1 hr
0.434	r/hr @ 10^{4} sec	2.74	r/hr @ 10^{5} sec

z	β Dose Rate	β/γ Ratio	β Dose Rate	β/γ Ratio
30 μ	18.33 rad/hr	42.	141.1 rad/hr	51.
100	12.12	28.	83.9	31.
300	7.71	18.	48.4	18.
1,000	3.75	8.6	17.7	6.5
3,000	1.21	2.8	3.4	1.2
10,000	0.06	0.1	0.0	0.0

CHARACTERISTICS OF THE GAMMA-RAY ENVIRONMENT PRODUCED BY FALLOUT FIELDS

R. L. French
Radiation Research Associates, Inc.
Fort Worth, Texas

ABSTRACT

The gamma-ray environment produced near the air-ground interface by ground-deposited fallout must be known in considerable detail for the evaluation of the radiation protection afforded by structures and for other purposes such as the study of the effects of fallout on biological systems. Two characteristics of critical importance are the energy distribution and the angular distribution of the gamma rays because the fraction of the exterior, or free-field, dose which penetrates to the interior of a structure is highly dependent upon them. Similarly, the energy and angular distributions influence the fraction of the free-field dose which may penetrate to the critical organs of an exposed person.

A number of measurements and calculations of the energy and angular distributions above fallout have been made but all of the results have significant limitations. In the calculations, the problem is usually highly idealized by assumptions such as an infinite plane source on a smooth ground surface. Measurements, on the other hand, suffer from angular resolution, and to a lesser extent, energy resolution problems. They include the effects of ground roughness and other perturbations peculiar to the location of the measurement. New measurements are, of course, precluded by the Limited Test Ban Treaty.

Examination and comparison of various calculated and measured energy and angular distribution data show reasonable consistency and indicate a very strong peak of uncollided gamma rays from just below the horizon and a more diffuse scattered component which comprises on the order of 15 percent of the total dose. Recent applications of these data to shield penetration calculations, however, show that relatively minor differences in the energy and angular distributions can lead to large differences in the fraction of the dose which penetrates to the interior.

Table I

Dose Rates 1 Meter Above Center of ^{137}Cs Source
70 Meters in Radius

(rad(tissue)/hr per source photon/cm^2-sec)

Component	Calculated	Measured
	Furrowed Surface	
Direct-Beam	3.517×10^{-7}	
Singly-Scattered	1.466×10^{-7}	
Adjustment for Multiple Scattering	2.506×10^{-7}	
Total	7.489×10^{-7}	8.430×10^{-7}
	Smooth Surface	
Direct-Beam	2.248×10^{-6}	
Singly-Scattered	2.397×10^{-7}	
Adjustment for Multiple Scattering	4.090×10^{-7}	
Total	2.897×10^{-6}	2.399×10^{-6}

The results of the first phase of the theoretical ground roughness study led to the recommendation that the next phase consist of an investigation of the role of the multiply-scattered component and the correlation of buried and mixed source calculations with some of the more recent experimental studies. The ultimate objective should be the selection of a single model and the establishment of parameters such as source depth for different types of terrain.

VI. GAMMA-RAY DEPTH-DOSE PATTERNS IN PHANTOM*

The objective of this investigation, which was initiated only two months ago, is to determine the gamma-ray depth-dose patterns in a phantom representative of the human body when exposed to the radiation environment produced by fallout fields and by selected arrangements of radioactive sources. Of particular interest is the determination of the differences in the depth-dose patterns produced by fallout and by radioactive source configurations intended to simulate fallout.

The phantom consists of a tissue-equivalent vertical right cylinder 60 cm in height and 30 cm in diameter. The center of the phantom is assumed to be 111.8 cm above a ground surface uniformly contaminated by fallout. The energy and angular distribution of the fallout and simulated fallout gamma rays incident upon the phantoms are being taken from the Monte Carlo calculations described in Sections II and III.

The chief mathematical tool being used to compute the depth-dose patterns is the COHORT Monte Carlo procedure.[28] A special FORTRAN procedure was prepared to calculate the uncollided gamma-ray components analytically. Preliminary calculations indicate that a minimum of approximately 50 percent of the dose at any point in the phantom is from photons which have suffered no previous collisions in the phantom.

*Based on work sponsored by the Armed Forces Radiobiology Research Institute, Defense Atomic Support Agency, under Contract No. DA-49-146-XA-479.

VII. MONTE CARLO STUDY OF BARRIER ATTENUATION FACTORS*

Today's Civil Defense fallout shielding technology[20] is based largely on simplified methods[29] developed from the results of rigorous calculations[8] which, in turn, are based on idealizations of the actual problems. Although a considerable amount of experimental and theoretical work has been carried out in recent years toward the evaluation of some of the approximations, the evaluations themselves often involve idealizations. For example, essentially all experiments have employed finite arrays of artificial sources of monoenergetic gamma rays to simulate the gamma rays from infinite plane fallout sources. Consequently there has been little direct verification of the basic results from which the simplified methods were developed.

To provide a more direct evaluation of the barrier attenuation data in current use, Radiation Research Associates is computing some of the more important cases using Monte Carlo techniques[2,19,28] which avoid certain idealizations required in the previous calculations. The Monte Carlo calculations include two cases of fundamental importance; 1) vertical wall barrier and 2) cylindrical wall barrier. In each case the energy and angular distribution of direct-beam and scattered gamma rays incident upon the barrier walls due to an infinite plane source on the ground surface will be considered. The energy and angular distributions of the incident gamma rays are the results of previous Monte Carlo calculations[1] which consider the effect of the air/ground interface. Concrete will be used as the barrier material.

The vertical wall barrier attenuation data given in Reference 8 were computed with the moments method, a method which has been used with great success in infinite medium calculations. The restriction of the moments method to infinite medium problems, however, leads to possible shortcomings in the barrier attenuation data since the gamma

*Based on work funded by the Office of Civil Defense through the United States Naval Radiological Defense Laboratory under Contract No. N0022866C0910.

radiation transport (both in the air/ground medium before reaching the barrier and the transport in the barrier) required idealization of the problem. Implicit in the infinite medium treatment is the restriction to a single material. Water was used to represent both air and ground and the barrier material itself was taken to be water. Other simplifications in the calculations included the neglect of energy degradation prior to striking the barrier. Results for a cylindrical barrier are generated from the slab barrier results by a geometrical transformation given in Reference 29.

The Monte Carlo calculations incorporate the individual material compositions of the air, the ground and the barriers. Material interface effects are included in the calculations and no compromise is necessary in handling the energy and angular distribution of the radiation. The Monte Carlo approach allows direct generation of results for the cylindrical barrier so that use of a geometric transformation is required as was the case for the moments method calculations. Comparisons of the Monte Carlo results with the previous results for slab and cylindrical barriers should help provide a basis for deciding whether the Civil Defense fallout shielding technology should continue to build from the old basic calculations or whether new results should be generated.

VIII. SUMMARY

Recent and current research projects at Radiation Research Associates encompass many of the numerous radiation transport problems involved in the determination of the characteristics of the gamma-ray environment produced by fallout and in the consideration of these characteristics in fallout shielding and radiobiology studies. The important characteristics of the radiation field for most purposes are the energy and angular distributions of the gamma-ray. These distributions are particularly important if penetration through appreciable amounts of material is involved.

Although the energy and angular distributions produced by fallout are known, or can presently be calculated with what appears to be reasonable accuracy for idealized situations where the source energy spectrum is known and the ground surface is smooth, it must be acknowledged that the exact amount of uncertainty in such calculations has not been established. Even in terms of the total dose above a plane isotropic ^{60}Co source, there are discrepancies on the order of 10 percent among various measurements and calculations.

The best choice of a source energy spectrum for a particular case is not too clear. The analysis of the enclosure shield experiment, which involved penetrations on the order of 2 to 6 relaxation lengths, indicated that the results obtained using various theoretical and experimental energy spectra varied widely. Of particular importance was the observation that the Nelms and Cooper fission product decay spectra,[3] which is incorporated into most Civil Defense barrier attenuation data, were not among those spectra which seemed to produce the best overall results for the enclosure shields. Although the different spectra did not give consistent dose transmission factors for the shields, they were reasonably consistent in indicating the time dependence of the transmission factors.

The nature of ground roughness effects is being determined in some detail through current theoretical and experimental efforts and there are indications that these effects may be accounted for by relatively simple methods. Further study is required in this area, however, before the methods can be definitized.

Fallout simulation studies indicate that either extended or compact configurations of common radioactive sources can give good simulation of most aspects of the fallour gamma-ray environment except the energy distribution. Studies are currently underway to determine the extent to which the depth-dose patterns in phantoms are influenced by the discrepancies in the energy spectra.

REFERENCES

1. R. L. French, Health Physics 11, 369 (1965).

2. D. G. Collins, Utilization Instructions for General Application of the LO5 Monte Carlo Procedure, RRA-T44 (1964).

3. Ann T. Nelms and J. W. Cooper, Health Physics 1, 427 (1959).

4. Gladys White Grodstein, X-ray Attenuation Coefficients from 10 KeV to 100 MeV, National Bureau of Standards Circular 583 (1957) with supplement (159).

5. R. L. Rexroad and M. A. Schmoke, Scattered Radiation and Free-Field Dose Rates from Distributed Cobalt-60 and Cesium-137 Sources, NDL-TR-2 (1960).

6. C. L. Schlemn, et al., Scattered Gamma Radiation Measurements from a Co^{60} Contaminated Field, AFSWC-TN-59-6 (1959).

7. E. T. Clark, Scattering of Gamma Rays at an Air-Ground Interface, unpublished paper (1965).

8. L. V. Spencer, Structure Shielding Against Fallout Radiation from Nuclear Weapons, NBS Monograph 42 (1962).

9. R. L. Mather, et al., Health Physics 8, 245 (1962).

10. R. L. French, A Comparative Study of Radioactive Source Arrangements for Simulating Fallout Gamma Radiation Fields, RRA-T45 (1964).

11. R. L. French, Simulation of Fallout Gamma Radiation Fields by Monoenergetic Plane Isotropic Sources, RRA-M51 (1965).

12. Development of a Fallout Simulator, Armed Forces Radiobiology Research Institute, Physical Sciences Report 1-63 (1963).

13. C. M. Cialella, et al., "Shielding Effectiveness of Enclosure Shields in a Fallout Field," POR-2221 (1963). (Confidential)

14. R. L. French, et al., An Analysis of the Performance of Enclosure Shields in a Real Fallout Field, RRA-T55 (1965).

15. Rolf Björnerstedt, Arkiv for Fysik 16, 293-313 (1959).

16. F. M. Tomnovec, et al., The Effect of a Changing Gamma-Ray Fallout Spectrum on the Ground Roughness Factor, USNRDL-TR-915 (1965).

17. C. Sharp Cook, Health Physics 4, 42-51 (1960).

18. C. M. Huddleston, et al., Health Physics 11, 537-548 (1965).

19. M. B. Wells, Monte Carlo Multilayer Slab Geometry Shielding Code C-18, FZK-134-3 (1961).

20. Design and Review of Structures for Protection From Fallout Gamma Radiation, Department of Defense, Office of Civil Defense, PM-100-1 Interim Edition (1965).

21. C. E. Clifford, Effects of Ground Roughness on the γ Dose from Cs^{137} Contamination, DRCL Report No. 401 (1963).

22. B. W. Shumway, USNRDL, private communications (1965, 1966).

23. R. L. French and L. Olmedo, A Preliminary Investigation of Simplified Methods for Calculating the Effects of Ground Roughness on the Gamma-Ray Environment Above Fallout, RRA-T61 (to be published).

24. C. F. Ksanda, et al., Gamma Radiation from a Rough Infinite Plane, USNRDL-TR-108 (1956).

25. C. F. Ksanda, et al., Gamma Radiation from Contaminated Planes and Slabs, USNRDL-TM-27 (1955).

26. C. E. Clifford, Can. J. Phys. 42, 2373 (1964).

27. C. Eisenhauer, Health Physics 9, 503 (1963).

28. M. B. Wells and C. F. Malone, A Monte Carlo Procedure for Radiation Transport and Heating Studies, FZK-156 (1962).

29. C. Eisenhauer, An Engineering Method for Calculating Protection Afforded by Structures Against Fallout Radiation, NBS Monograph 76 (1964).

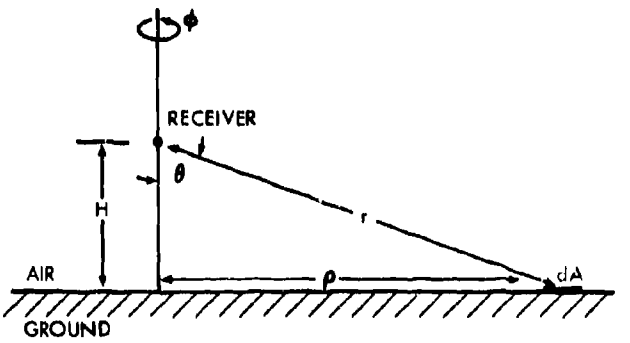

Fig. 1. Source and Receiver Geometry

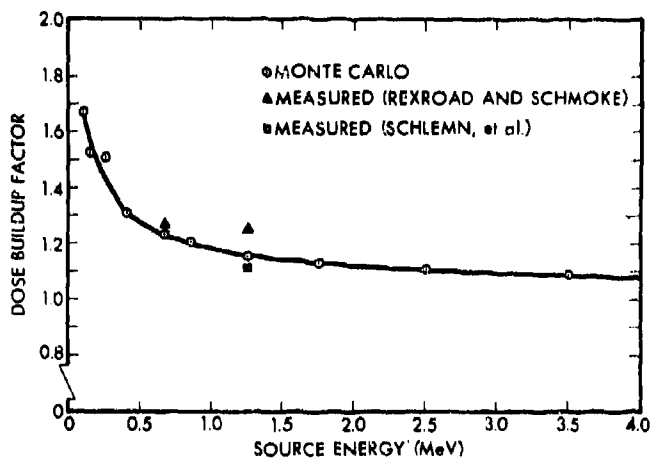

Fig. 2. Gamma Dose Buildup Factors for Receiver in Air 3 Feet Above Infinite Plane Isotropic Source on Ground

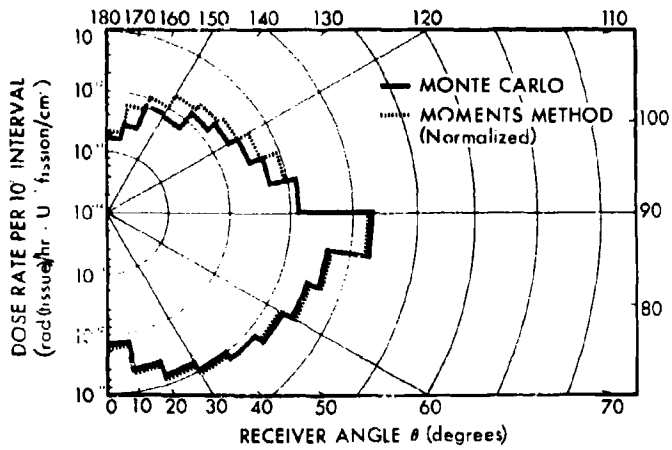

Fig. 3. Comparison of Monte Carlo and Moments Method Gamma-Ray Dose Rate Angular Distribution from 1.12 Hour Fallout

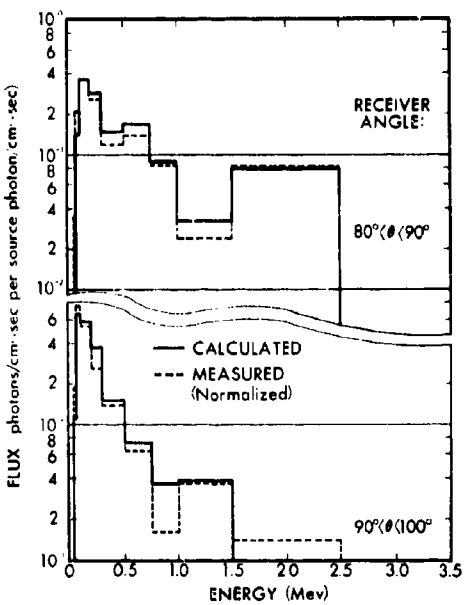

Fig. 4. Comparison of Calculated and Measured Gamma-Ray Energy Spectra 3 Feet Above 9 Day Fallout

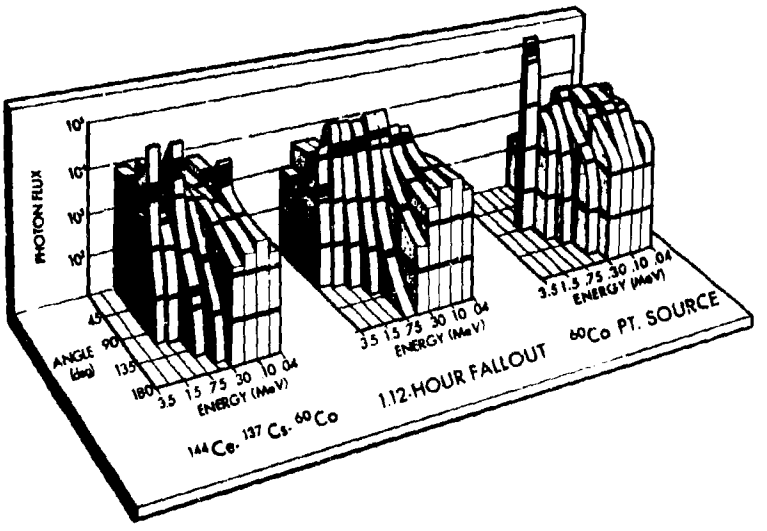

Fig. 5. Comparison of Flux Energy and Angular Distributions 3 Feet Above 1.12 Hour Fallout and Simulated Fallout

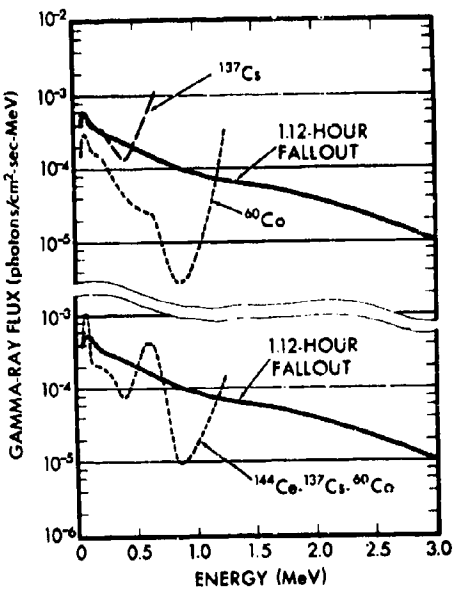

Fig. 6. Differential Energy Spectra 3 Feet Above Infinite Plane Source

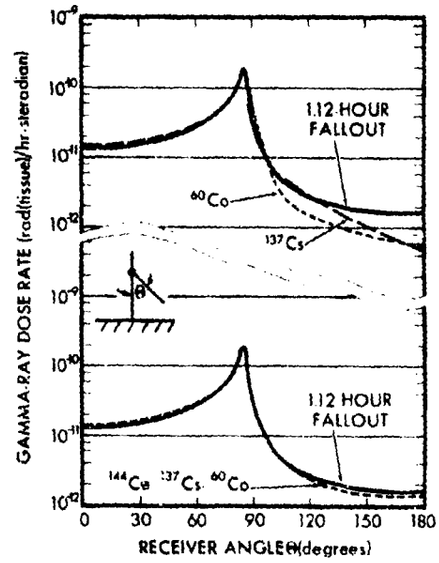

Fig. 7. Differential Dose Angular Distribution 3 Feet Above Infinite Plane Source

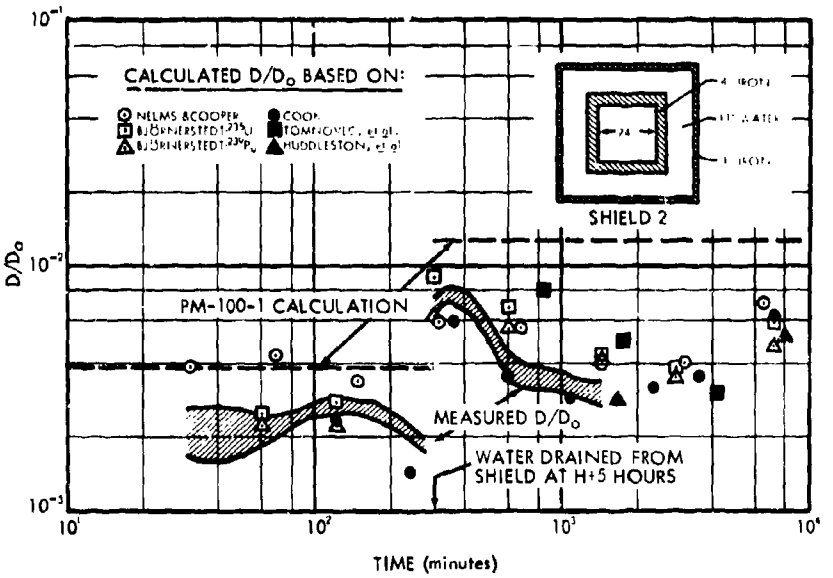

Fig. 8. Calculated and Measured Dose Transmission Factors for Cubical Enclosure Shield 2

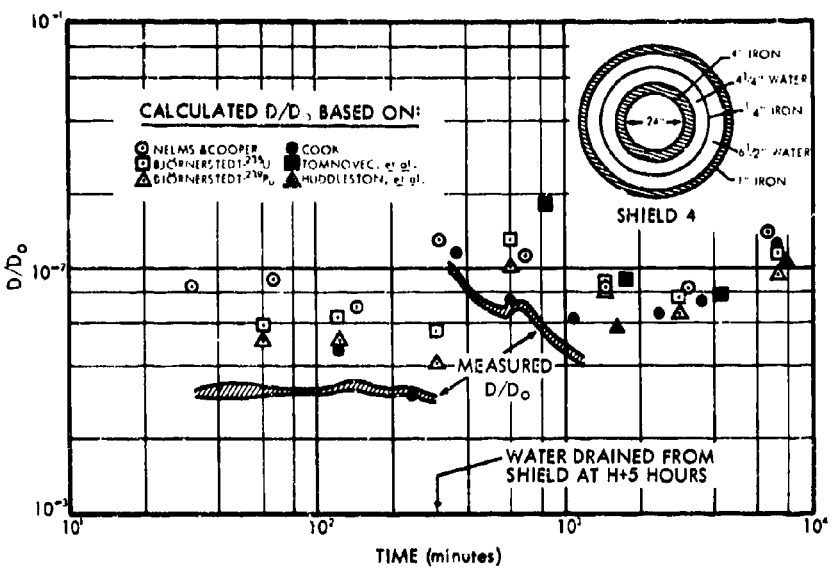

Fig. 9. Calculated and Measured Dose Transmission Factors for Spherical Enclosure Shield 4

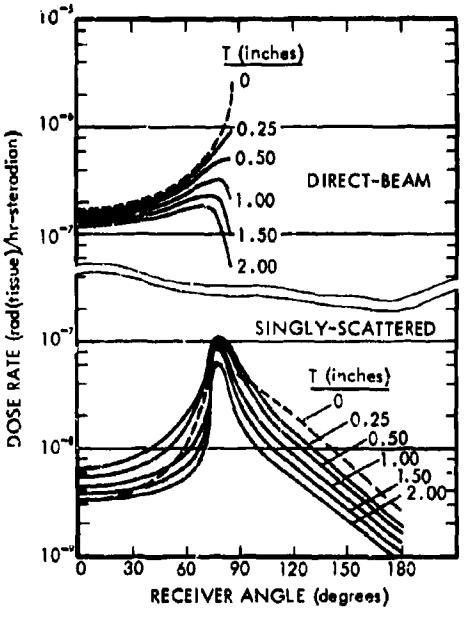

Fig. 10. Angular Distribution of Gamma-Ray Dose Rate 3 Feet Above 1.25 MeV Source at Depth T Below Ground Surface

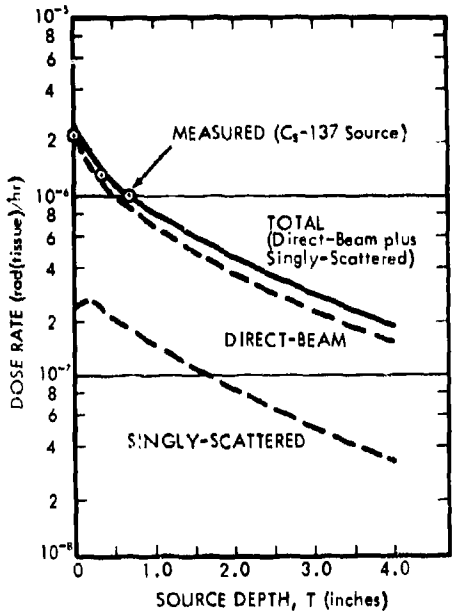

Fig. 11. Gamma-Ray Dose Rates 3 Feet Above 0.67 MeV Source at Depth T Below Ground Surface

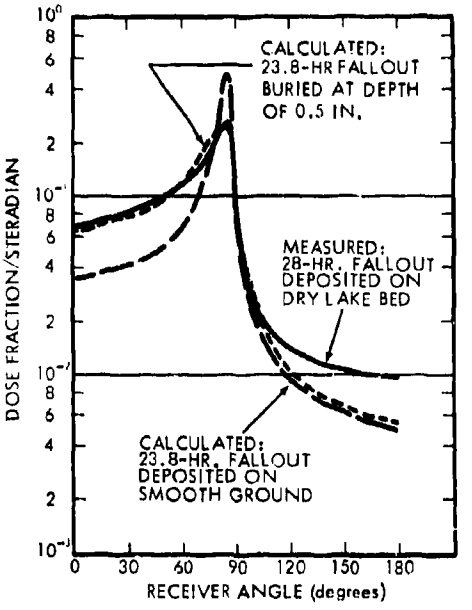

Fig. 12. Comparison of Measured and Calculated Dose Angular Distributions Above Fallout Deposited on a Dry Bed

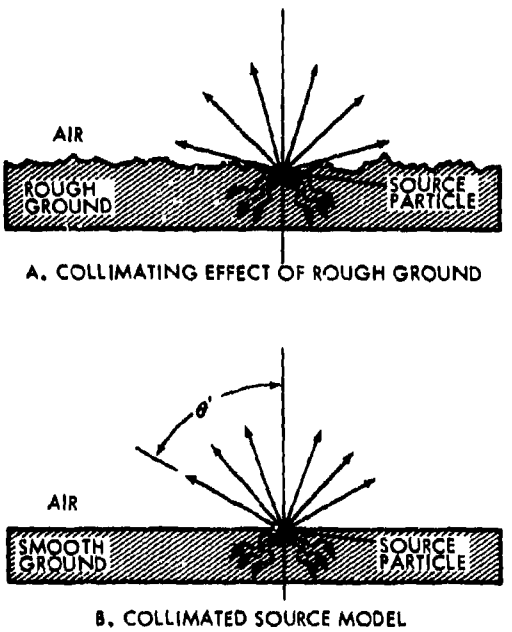

Fig. 13. Collimated Source Model for Simulating Ground Roughness Effects

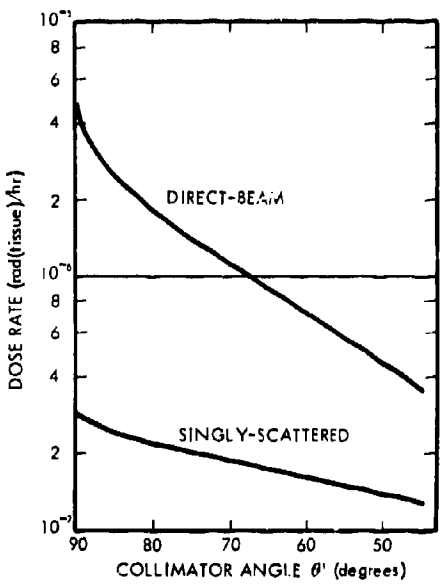

Fig. 14. Gamma-Ray Dose Rates 3 Feet Above Collimated 1.25 MeV Source

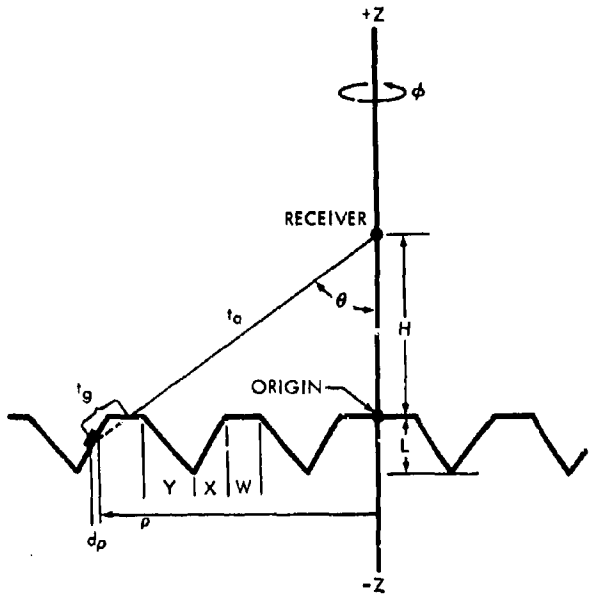

Fig. 15. Geometry of Furrowed-Surface Ground Roughness Model

INTENSITY--ACTIVITY RELATIONS FOR SHOT SMALL BOY

P. D. LaRiviere, S-K Yu and C. F. Miller

Stanford Research Institute
Menlo Park, California

ABSTRACT

An analysis of the relationship of gamma exposure rate to fission density and ionization activity of fallout samples from event Small Boy was made. The results indicate that, over the fallout region sampled, the fractionation of radionuclides was such that only ~30% of the gamma ionization strength per refractory fission of unfractionated fission products was exhibited. The combined effects of instrument response characteristics and terrain roughness were seen to further depress expected exposure rates at 1 hour after burst by an average factor of 0.72.

REFERENCES

1. Miller, C. F., and J. D. Sartor, Small Boy Shot Fallout Research Program in Radioactive Fallout From Nuclear Weapons Tests. Proceedings of the Second Conference, Germantown, Md., Nov. 3-6, 1964. Alfred W. Klement, Jr., Editor. AEC Symposium Series 5, Nov. 1965.

2. Miller, C. F., The Ionization Rate and Photon Pulse Decay of Fission Products from the Slow-Neutron Fission of U235. USNRDL-TR-247, U.S. Naval Radiological Defense Laboratory, Aug. 1958 (Unclassified).

3. Mackin, J. L., USNRDL, Private Communication, April 1966.

4. Miller, C. F., Analysis of Fallout Data, Part III. The Correlation of Some CASTLE Fallout Data from Shots 1, 2 and 3. USNRDL-TR-222, U.S. Naval Radiological Defense Laboratory, May 1958. (SECRET RESTRICTED DATA).

5. LaRiviere, P. D., J. D. Sartor, W. B. Lane, and K. H. Larson, Fallout Collection and Gross Sample Analysis (U), Project 2.9, Operation SUN BEAM, Shot Small Boy, POR-2215, U.S. Naval Radiological Defense Laboratory, Oct. 1964 (SECRET RESTRICTED DATA).

6. Freiling, E. C., L. R. Bunney, and F. K. Kawahara, Physicochemical and Radiochemical Analysis (U), Project 2.10, Operation SUN BEAM, Shot Small Boy, POR-2216, U.S. Naval Radiological Defense Laboratory, Oct. 1964 (SECRET RESTRICTED DATA).

7. Bouton, E. H., et al., Radiological Surveys (U), Project 2.8, Operation SUN BEAM, Shot Small Boy, POR-2266, U.S. Army Nuclear Defense Laboratory, Oct. 1964 (SECRET RESTRICTED DATA).

8. LaRiviere, P. D., H. Lee, and K. H. Larson, Ionization Rate Measurements (U), Project 2.11, Operation SUN BEAM, Shot Small Boy, POR-2217, U.S. Naval Radiological Defense Laboratory, undated (CONFIDENTIAL).

9. Yu, Oliver S-K, Study on the Mass Contour Ratio, SRI Project No. _____. Stanford Research Institute report in preparation.

10. Strope, W. E., Evaluation of Countermeasure System Components and Operational Procedures, Project 32.3, Operation PLUMBBOB, WT-1464, U.S. Naval Radiological Defense Laboratory, Sept. 1959 (Unclassified).

11. Miller, C. F., Biological and Radiological Effects of Fallout from Nuclear Explosions, Chapter 1: The Nature of Fallout. Chapter 2: Formation of Fallout Particles. SRI Project No. IMU-4536, Stanford Research Institute, March 1964 (Unclassified).

12. Bolles, R. C., and N. E. Ballou, Calculated Activities and Abundances of U235 Fission Products, USNRDL-456, U.S. Naval Radiological Defense Laboratory, Aug. 1956 (Unclassified).

13. Miller, C. F., Fallout and Radiological Countermeasures, Volume I, SRI Project No. IM-4021, Stanford Research Institute, Jan. 1963 (Unclassified).

14. Crocker, G. R., The Effect of Radionuclide Fractionation on the Normalization Factor for Fallout Fields, USNRDL-TR-892, U.S. Naval Radiological Defense Laboratory, Aug. 1965 (Unclassified).

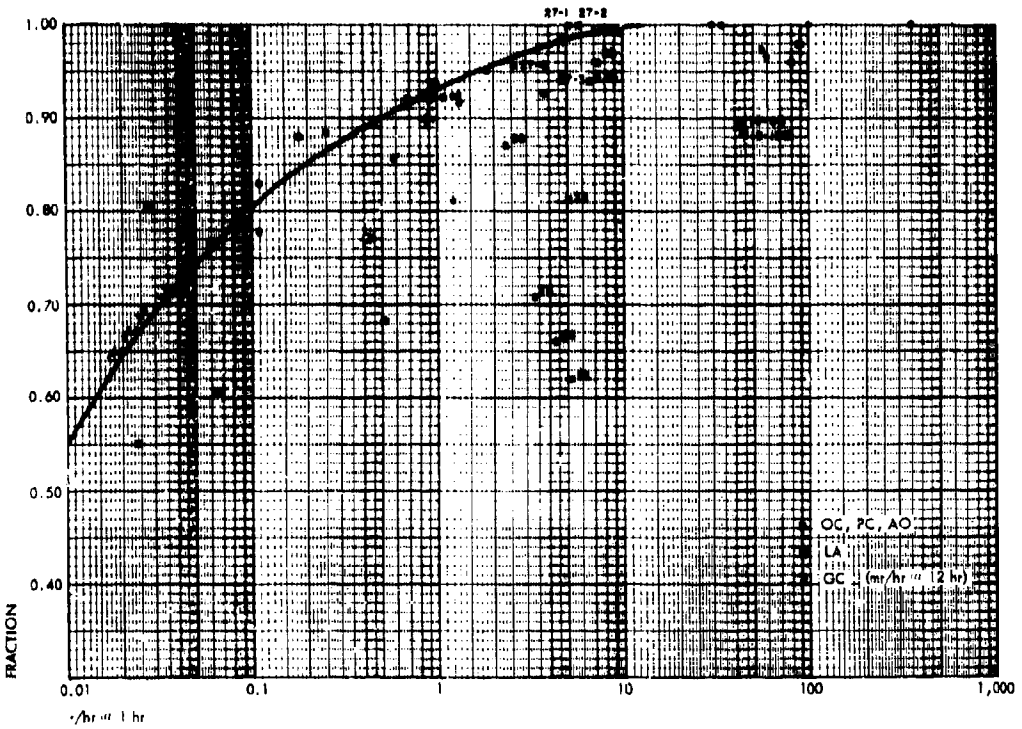

Fig. 1. Fraction of Sample Recovered from Project 2.9 Collectors

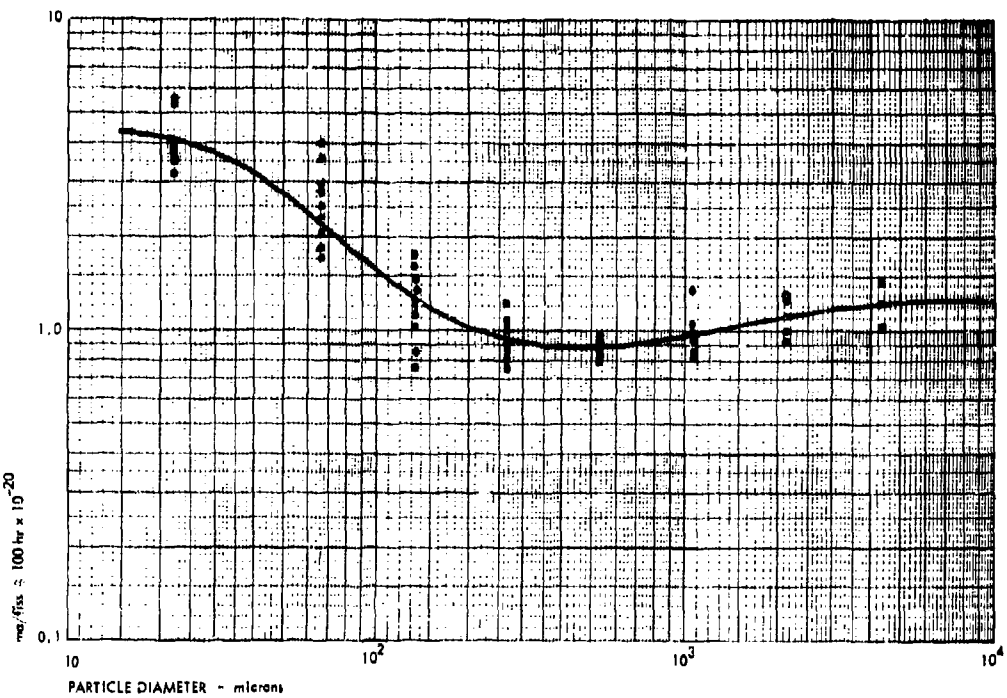

Fig. 2. Variation of ma/fission @ 100 hr with Particle Size

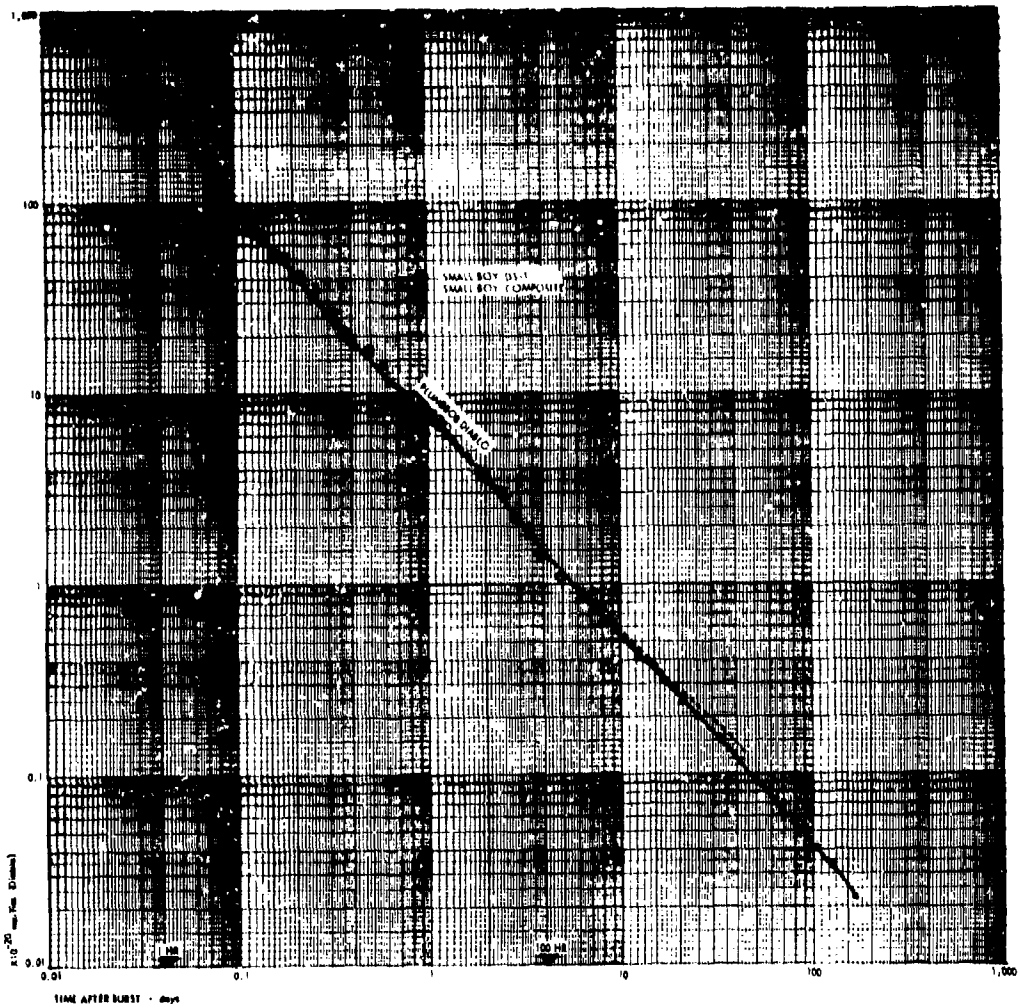

Fig. 3. Decay Rates of Diablo and Small Boy Samples in the 4 π Ion Chamber

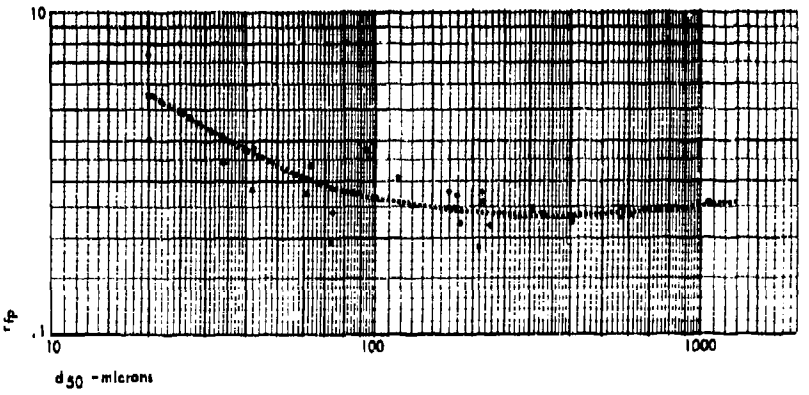

Fig. 4. Variation of Gross Fractionation Number with Median Size of Fallout Samples